Ph.D. Course on *Vorticity, Vortical Flows and Vortex-Induced Vibrations*
Technical University of Denmark, Copenhagen, Denmark
vortex.compute.dtu.dk
August 26-30, 2019

Bluff Body Wakes I: Introduction

Kerry Hourigan
Fluids Laboratory for Aeronautical and Industrial Research
Monash University, Melbourne, Australia
Otto Mønsted Guest Professor, Technical University of Denmark

MONASH University

FLAIR
Fluids Laboratory for Aeronautical and Industrial Research

Reading Material

Barkley, D. & Henderson, R.D., Three-dimensional Floquet stability analysis of the wake of a circular cylinder, 322, 215-241, 1996.

Bearman, P.W., On vortex shedding from a circular cylinder in the critical Reynolds number regime, J. Fluid Mech., 37, 577-585, 1969.

Bloor, M.S., The transition to turbulence in the wake of a circular cylinder, J. Fluid Mech. 19, 290, 1964.

Cimbala,J.M., Nagib, H.M. & Roshko, A., Large structure in the far wakes of two-dimensional bluff bodies, J. Fluid Mech., 190, 265-298, 1988.

Johnson, S.A., Thompson M.C. & Hourigan, K., Predicted low frequency structures in the wake of elliptical cylinders, European Journal of Mechanics B/Fluids, 23, 229-239, 2004.

Karasudani, T. & Funakoshi, M., Evolution of a vortex street in the far wake of a cylinder, Fluid Dynamics Research, 14, 331-352, 1994.

Norberg, C., An experimental investigation of the flow around a circular cylinder: Influence of aspect ratio, J. Fluid Mech. 258, 287, 1994.

Prasad, A. & Williamson, C.H.K., The instability of the shear layer separating from a bluff body, J. Fluid Mech. 434, 235, 1997.

Radi, A., Thompson, M.C., Sheridan, J. & Hourigan, K., From the circular cylinder to the flat plate wake: the variation of Strouhal number with Reynolds number for elliptical cylinders, Physics of Fluids, 25, 101706, 2013.

Roshko, A., On the drag and shedding frequency of two-dimensional bluff bodies, NACA Technical Report No. 3169 (1954).

Taneda, S., Downstream Development of the Wakes behind Cylinders, Journal of the Physical Society of Japan, Volume 14, Issue 6, pp. 843-848,1959.

Thompson, M.C., Hourigan, K. & Sheridan, J., Three-dimensional instabilities in the wake of a circular cylinder, International Journal of Experimental Heat Transfer, Thermodynamics, and Fluid Mechanics, 12, 190-196, 1996.

Thompson, M.C., Radi, A., Rao, A., Sheridan, J. & Hourigan, K., Low-Reynolds-number wakes of elliptical cylinders: from the circular cylinder to the normal flat plate, Journal of Fluid Mechanics, 751, 570-600, 2014.

Wei, T. & Smith, C.R., Secondary vortices in the wake of circular cylinders, J. Fluid Mech. 169, 513, 1986.

Williamson, C.H.K., Vortex Dynamics in the Cylinder Wake, Annual Review of Fluid Mechanics, 28, 477-539, 1996.

Williamson, C.H.K. & Prasad, A., A new mechanism for oblique wave resonance in the ‘natural’ far wake, J. Fluid Mech., 256, 269-313, 1993.

Zdravkovich, M., Flow around Circular Cylinders Volume 1: Fundamentals, 1st ed. (Oxford University Press, Oxford, 1997).

Lecture Objectives

Learn:

The importance of bluff body flows

The different instabilities and transitions in the wakes of generic bodies

Methods of predicting wake instability frequencies and wavelengths

υ

Overview

- **Generic bluff bodies: The sphere and circular cylinder**
  - Different bifurcation scenarios
  - Different instabilities in the wake
- **Conclusions**

Importance of Bluff Body Flows

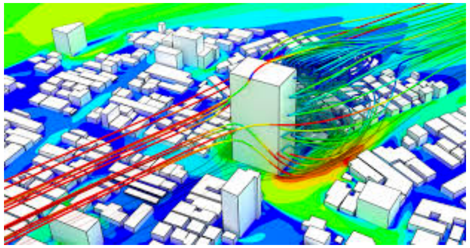

Flows around buildings
www.simscale.com/blog/2018/07/working-in-wind-engineering/

Towers of wind turbines
nautil.us/issue/37/currents/fish-school-us-on-wind-power-rp

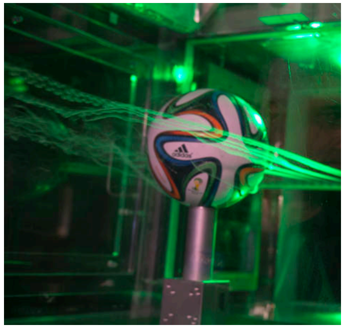

Flow around sports balls
www.nasa.gov/content/nasa-turns-world-cup-into-lesson-in-aerodynamics/

Flow around humans
https://www.mr-cfd.com/portfolio-item/airflow-around-the-human-body/

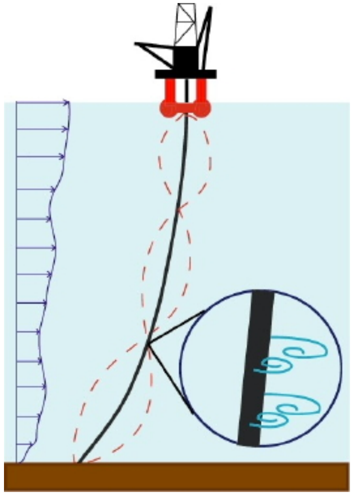

Flow offshore risers
www3.imperial.ac.uk/vortexflows/research/fluidstruct/vivofflexiblestructures

Vehicle Aerodynamics
www.monashmotorsport.com/undertray/

The flow past spheres & circular cylinders

Important parameter: Reynolds number $Re = U D / \upsilon$

U is flow velocity, D is body "diameter", υ is kinematic viscosity

- **Sphere:**
  - $0 < Re < 211$: Steady axisymmetric wake

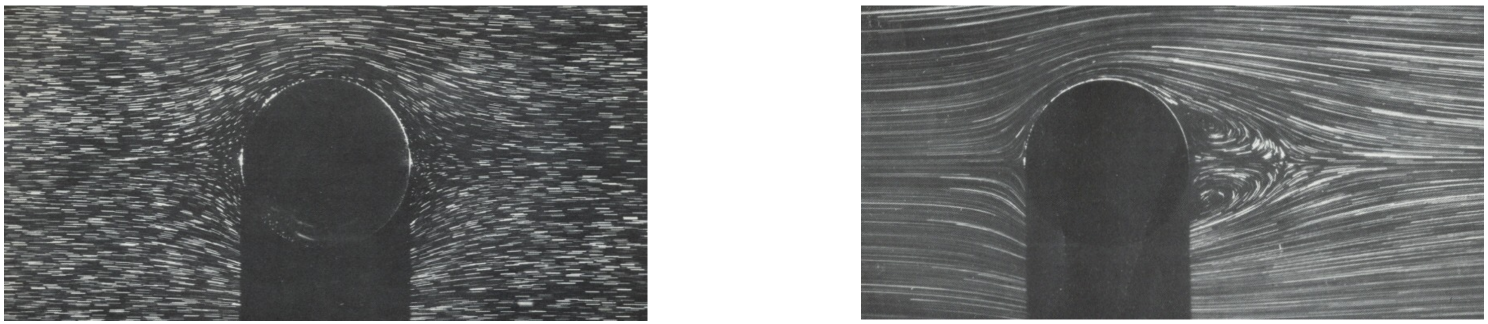

Attached flow (left, *Re* = 0.1) & separated flow (right, *Re* = 56.5) past a sphere

Photographs: M. Payard & M. Coutanceau (Van Dyke 1982)

  - $Re > 272$: Hairpin shedding, turbulence, etc.

The flow past spheres & circular cylinders

- **Sphere:**
  - 0 < *Re* < 211: Steady axisymmetric wake
  - *Re* = 211: Regular supercritical bifurcation (azimuthal mode number *m* = 1)
  - 211 < *Re* < 272: Steady non-axisymmetric wake
  - *Re* = 272: Supercritical Hopf bifurcation (*m* = 1)
  - *Re* > 272: Hairpin shedding, turbulence, etc.

The flow past spheres & circular cylinders

- **Sphere:**
  - $0 < Re < 211$: Steady axisymmetric wake

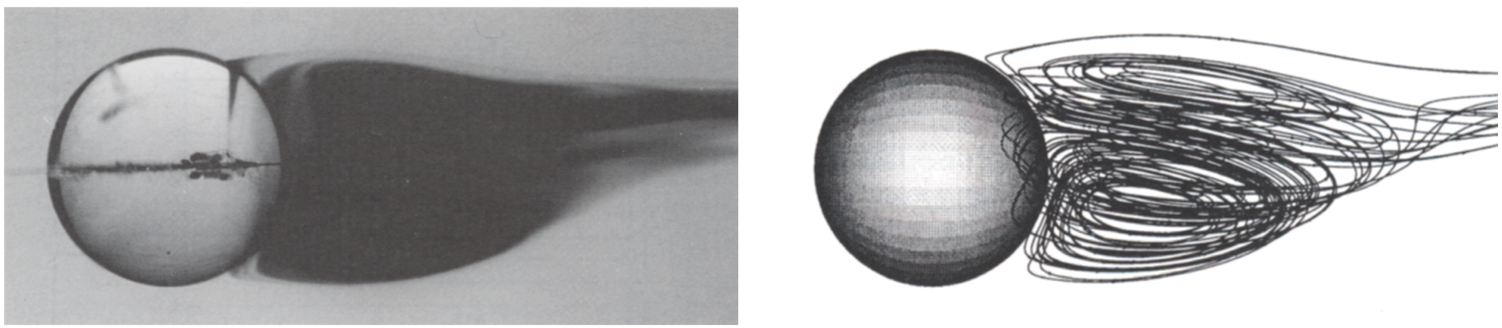

Steady non-axisymmetric wake behind a sphere at Re = 250

Johnson & Patel (1999)

  - $Re > 272$: Hairpin shedding, turbulence, etc.

The flow past spheres & circular cylinders

- **Sphere:**
  - 0 < *Re* < 211: Steady axisymmetric wake
  - *Re* = 211: Regular supercritical bifurcation (azimuthal mode number *m* = 1)
  - 211 < *Re* < 272: Steady non-axisymmetric wake
  - *Re* = 272: Supercritical Hopf bifurcation (*m* = 1)
  - *Re* > 272: Hairpin shedding, turbulence, etc.

The flow past spheres & circular cylinders

- **Sphere:**
  - 0 < *Re* < 211: Steady axisymmetric wake

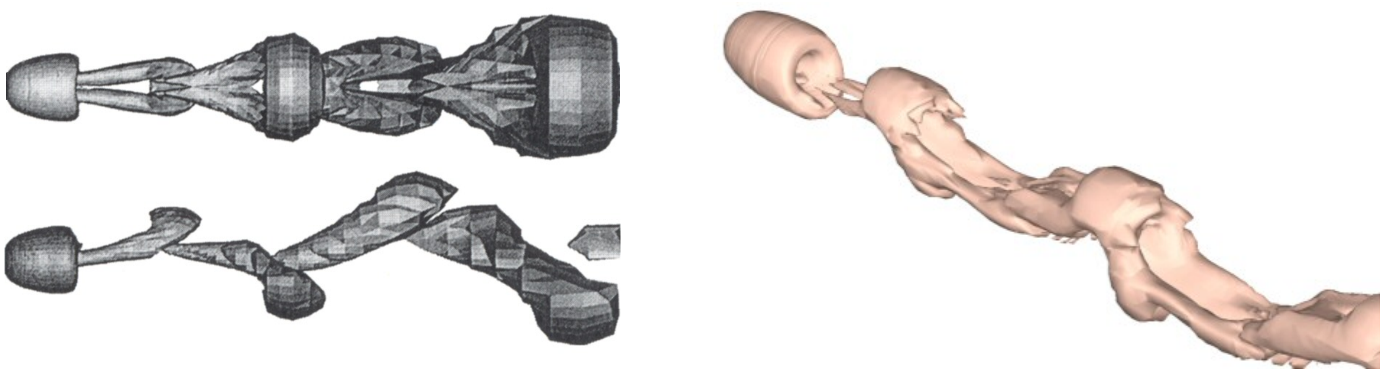

Computed unsteady wakes behind a sphere at *Re* = 300

Left: Johnson & Patel (1999), Right: Sheard *et al.* (JFM, 2004)

  - *Re* > 272: Hairpin shedding, turbulence, etc.

The flow past spheres & circular cylinders

- **Cylinder:**
  - 0 < *Re* < 47: Steady 2D wake
  - *Re* = 47: Supercritical Hopf bifurcation
  - 47 < *Re* < 180: Periodic 2D vortex street
  - *Re* = 180: Subcritical Mode A inst. ($\lambda_d \approx 4d$)
  - *Re* > 180: 3D vortex shedding, secondary Mode B instability, turbulent transitions, etc.

The flow past spheres & circular cylinders

- **Cylinder:**
  - – 0 < *Re* < 47: Steady 2D wake
  - – *Re* = 47: Supercritical Hopf bifurcation
  - – 47 < *Re* < 180: Periodic 2D vortex street
  - – *Re* = 180: Subcritical Mode A inst. ($\lambda_d \approx 4d$)
  - – *Re* > 180: 3D vortex shedding, secondary Mode B instability, turbulent transitions, etc.

The flow past spheres & circular cylinders

- **Cylinder:**

2D vortex street behind a circular cylinder at *Re* = 140

Photograph: S. Taneda (Van Dyke 1982)

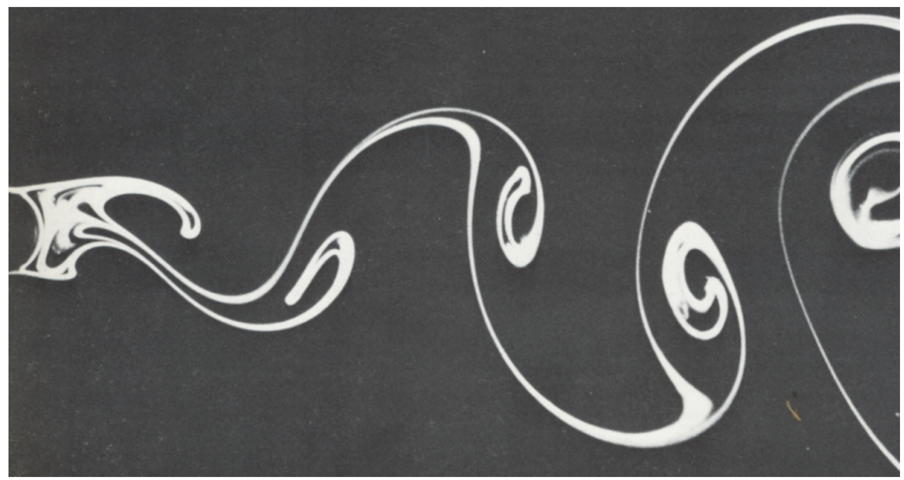

The circular cylinder is a canonical 2d bluff body

Non-rotating cylinder in a cross-flow: allée de Bénard-von Kármán

Reynolds number Re = Ud/v

Strouhal number St = fd/U

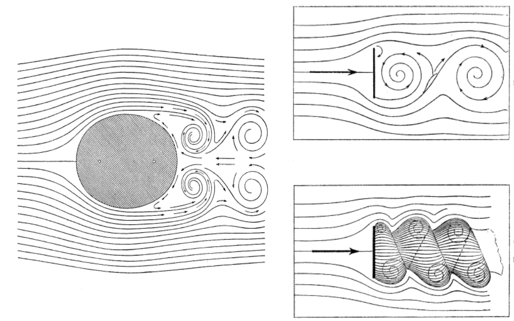

2d 3d

Mallock (1907)

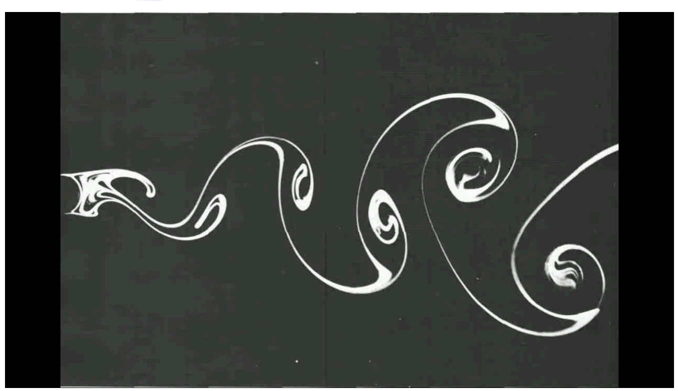

https://www.youtube.com/watch?v=3mULL6O6f38

A. Mallock, 1907: On the resistance of air. Proc. Royal Soc., A79, pp. 262–265.
H. Bénard, 1908: Comptes rendus de l'Académie des Sciences (Paris), vol. 147, pp. 839–842, 970–972.
T. von Kármán: and H. Rubach, 1912: Phys. Z., vol. 13, pp. 49–59.

Summary of large-scale transitions for a circular cylinder

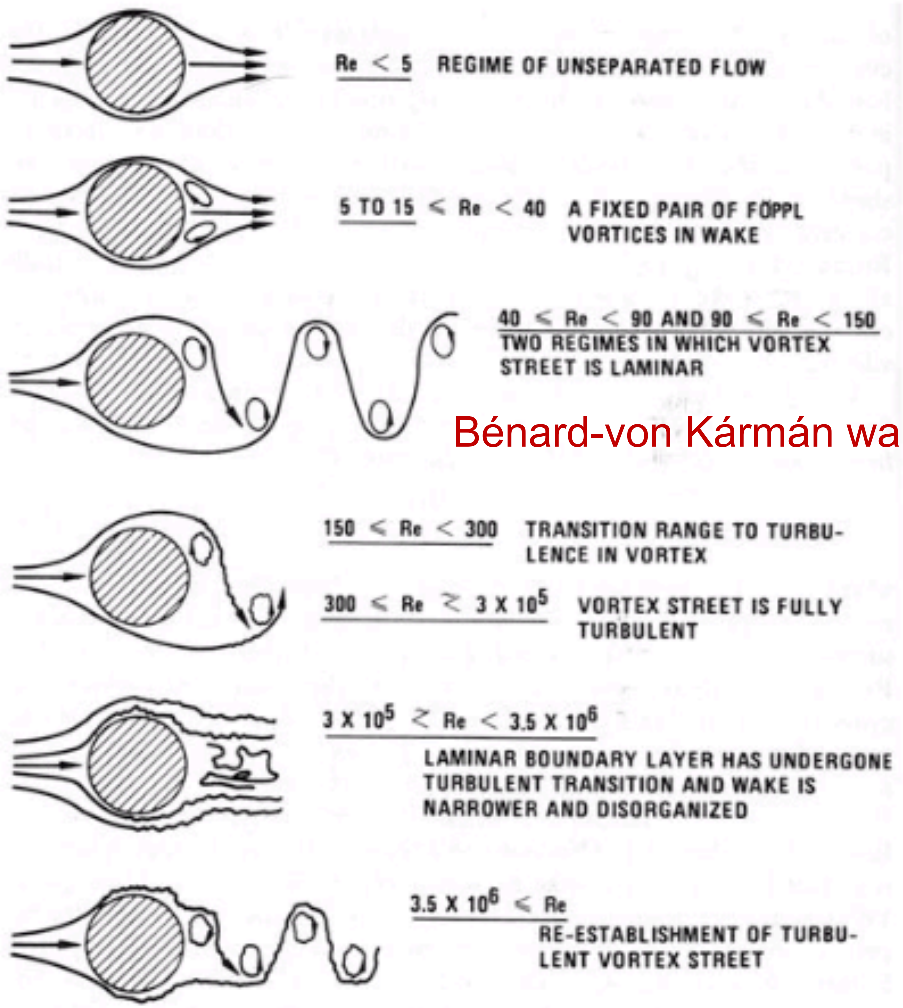

Fig. 3-2 Regimes of fluid flow across smooth circular cylinders (Lienhard, 1966).

Bénard-von Kármán wake

$R_d < 5$

$5\text{-}15 < R_d < 40$

$40 < R_d < 150$

$150 < R_d < 300$

Transition to turbulence

$300 < R_d < 3*10^5$

$3*10^5 < R_d < 3.5*10^6$

$3.5*10^6 < R_d$

Drag Coefficient for 2D bodies

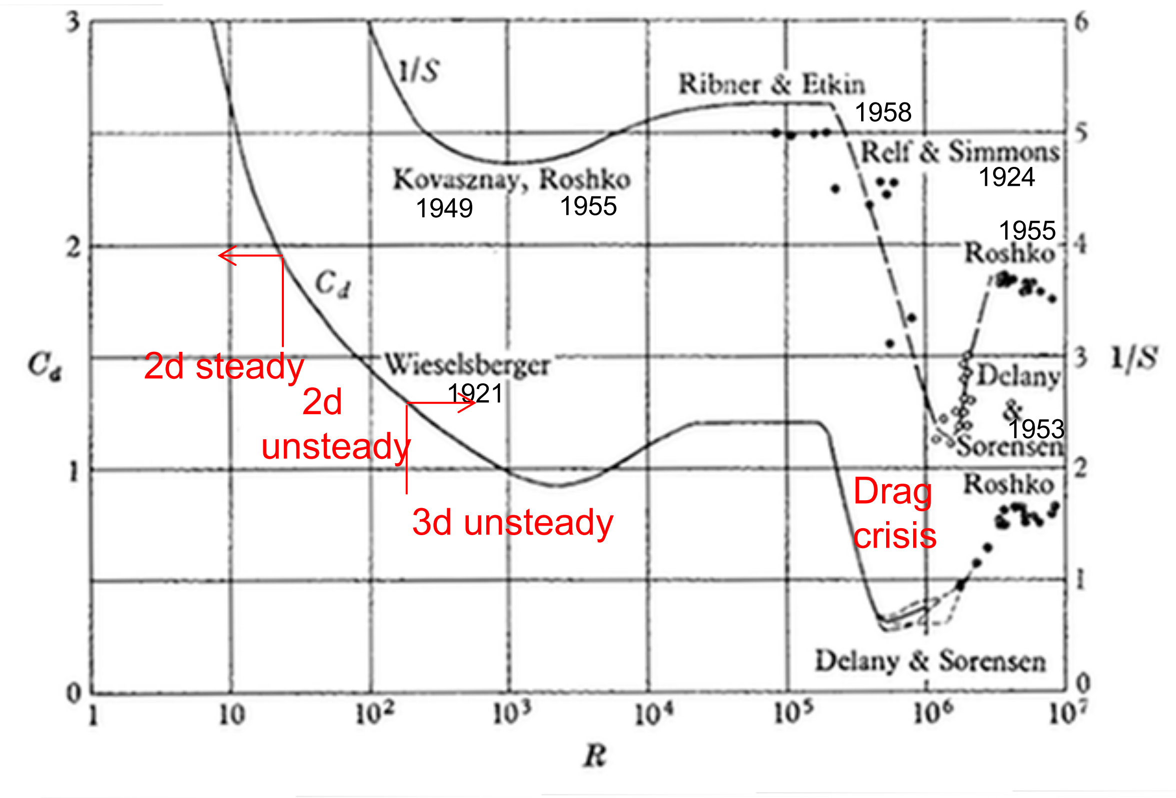

Drag coefficient and reciprocal of Strouhal number for flow past a Cylinder.
Roshko (JFM, 1961)

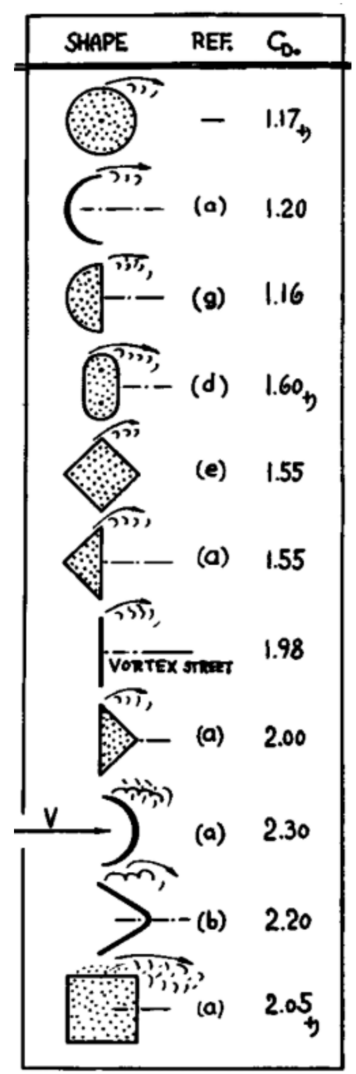

Drag coefficient at "turbulent" Re for various 2D shapes.
(Sighard Hoerner's Fluid Dynamic Drag, Chapter 3)

Drag Coefficient for 3D bodies

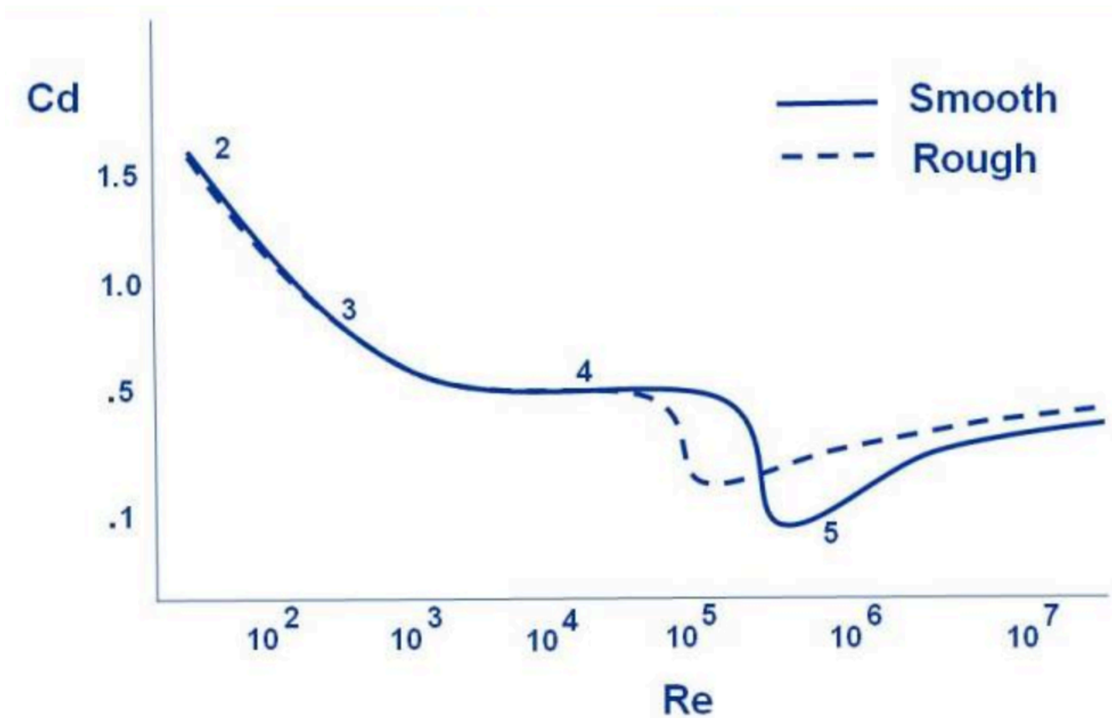

Drag coefficient for flow past a Sphere as a function of Reynolds number Re. (NASA)

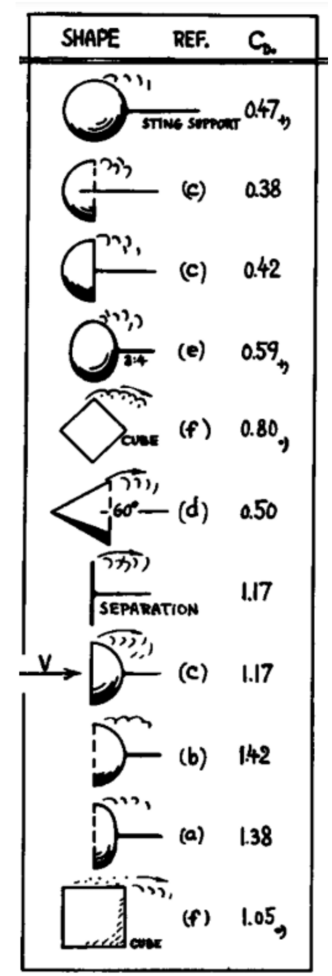

Drag coefficient at “turbulent” Re for various 3D shapes.
(Sighard Hoerner's Fluid Dynamic Drag, Chapter 3)

Wakes and transitions for a stationary circular cylinder

Steady 2d to unsteady 2d – global frequency selection

Circular Cylinder: 2D Instability

Different Approaches to determining stability

- **Steady base flow**
  - Undertake non-linear stability analysis
- **Time-mean velocity field**
  - Flow is saturated
  - Undertake linear stability analysis
- **Time-dependent field**
  - Flow perturbation

Barkley, Europhys. Lett. (2006)

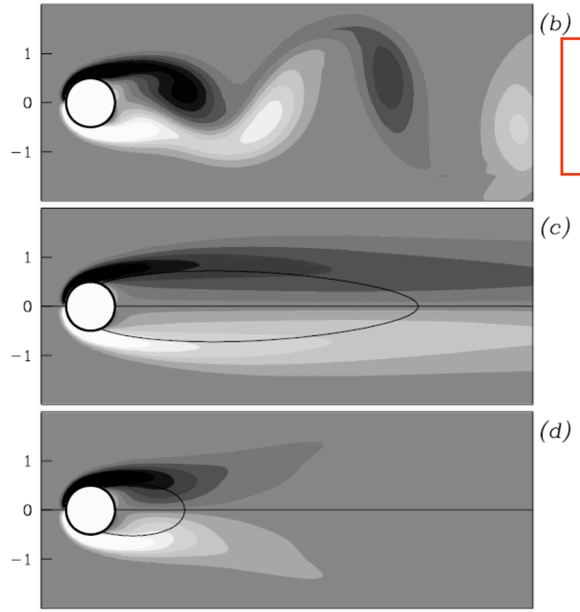

Vorticity field - cylinder wake
Re = 100

Unstable steady wake
Re = 100

Time-mean wake
Re = 100

How is Wake Frequency Selected?

- **Problem: *Wake absolutely unstable over a finite spatial range*.**
  - Prediction of frequency at any point in this range.
  - So what is the selected frequency?

- **There were three competing theories:**
  - **Monkewitz and Nguyen (1987)** proposed the *Initial Resonance Condition*
    - > The frequency selected corresponds to the predicted frequency at the point where the initial transition from convective to absolute instability occurs.
  - **Koch (1985)** proposed the *downstream resonance condition*.
    - > This states that it is the downstream transition from absolute to convective instability that determines the selected frequency.
  - **Pierrehumbert (1984)** proposed that the selection is determined by the point in the absolute instability range with the *maximum amplification rate*.

  - These theories are largely ad-hoc.

Selection of Wake Frequency - Saddle Point Criterion

- **Since then**
  - **Chomaz, Huerre, Redekopp (1991) & Monkewitz** in various papers have shown that the global frequency selection for (near) parallel flows is determined by the complex frequency of the saddle point in complex space, which can be determined by analytic continuation from the behaviour on the real axis.
  - This was demonstrated by the work of **Hammond and Redekopp (1997)**, who examined the frequency prediction for the wake from a square trailing edge cylinder.

Test Case - Flow over Trailing Edge Forming a Wake

- **Hammond and Redekopp (JFM 1997): use time-averaged profiles**

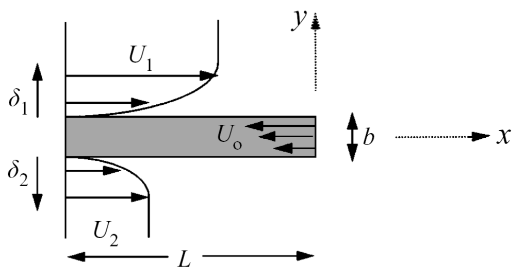

Linear theory assumptions

Is the wake parallel?

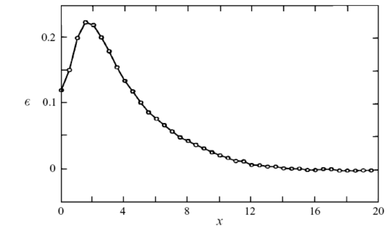

FIGURE 4. A measure of the non-parallel nature of the spatially developing wake at $Re = 160$.

Re=160

Frequency prediction with downstream distance

The real and imaginary components of the complex frequency is determined using both Orr-Sommerfeld (viscous) and Rayleigh (inviscid) solvers from velocity profiles across the wake.

Saddle Point Criterion: Prediction of preferred frequency is:

Parallel inviscid theory at Re=160 gives **0.1006**

Numerical simulation of (saturated) shedding at Re=160 gives **0.1000**.

Better than 1% accuracy!

Saddle point at $(x_{sr}, x_{si}) = (0.79, 0.078)$

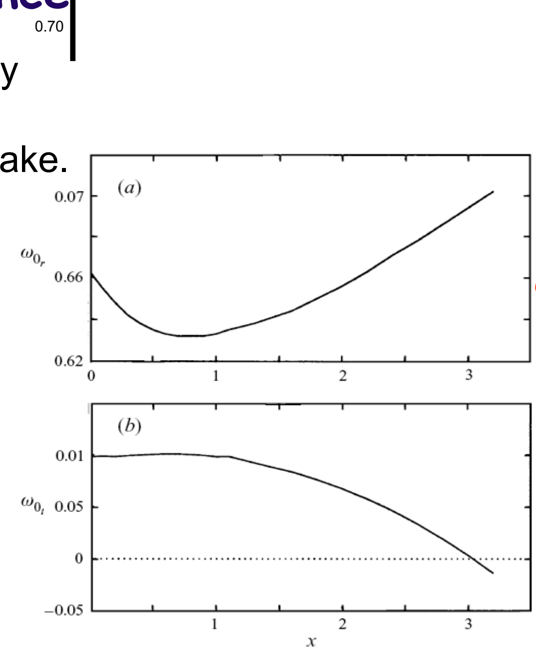

Predicted oscillation frequency

Predicted growth rate

FIGURE 5. (a) The absolute frequency and (b) the absolute growth rate for the wake at $Re = 160$.

Saddle Point Criterion

- Prediction of selected frequency:
  - Find saddle point in complex plane where group velocity is zero <u>and</u> growth rate if positive

$$\left.\frac{\partial \omega_0}{\partial x}\right|_{x=x_s} = 0. \qquad \omega_0(x_s) > 0$$

Here, both ω_0 and x are complex!

> Can use complex Taylor series + Cauchy-Riemann equations to project off the real axis (…the only place where you have data).

$$\omega_{0_r}(x_s) = \omega_{0_r}(x_r, x_i = 0) - \left.\frac{\partial \omega_{0_i}}{\partial x_r}\right|_{x_i=0} x_i + O(x_i^2),$$

$$\omega_{0_i}(x_s) = \omega_{0_i}(x_r, x_i = 0) + \left.\frac{\partial \omega_{0_r}}{\partial x_r}\right|_{x_i=0} x_i + O(x_i^2).$$

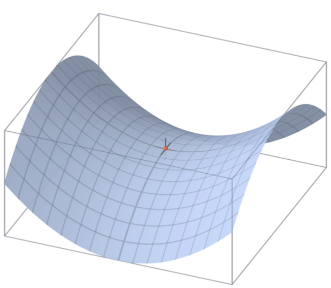

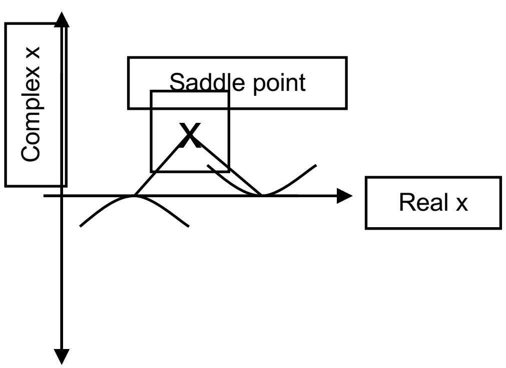

Frequency Prediction for a Circular Cylinder Wake

- **Numerical Stability Analysis based on Time-Mean Flow**
  - Extract velocity profiles across wake
  - Analyze using parallel stability analysis to predict Strouhal number

Re	St_{DNS}	St_{Glob}	St_{Ray}	$x_{\mathrm{saddle,Ray}}$	St_{MN}	St_{MNR}	St_{WB}
Two-dimensional wake							
100	0.1659	0.1639	0.1644	1.34	0.171*		0.1647
200	0.1970	0.1945	0.1972	1.05	0.194*		0.1945

DNS　　Rayleigh equation　　Experiments

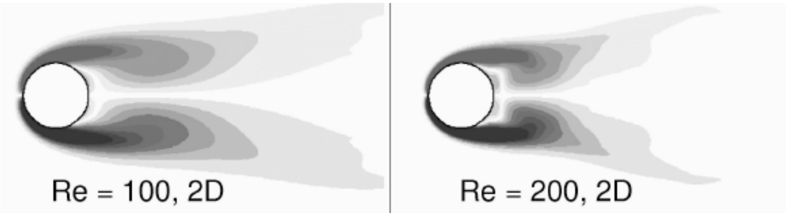

Inadequacy of Theory?

- **We need to know the time-mean flow (either by numerical simulation or running experiments) to compute the preferred wake frequency!**
  - Not necessarily a predictive tool but gives insight to wake stability…
- **Another option is to undertake a non-linear stability analysis on the steady base flow (when the wake is still steady - prior to shedding).**
  - This was done by Pier (JFM 2002).

Non-Linear Theory

- **Pier (JFM 2002) & Pier and Huerre (2001).**
  - Frequency selection based on the (imposed) steady cylinder wake using *non-linear theory*.

Absolute instability

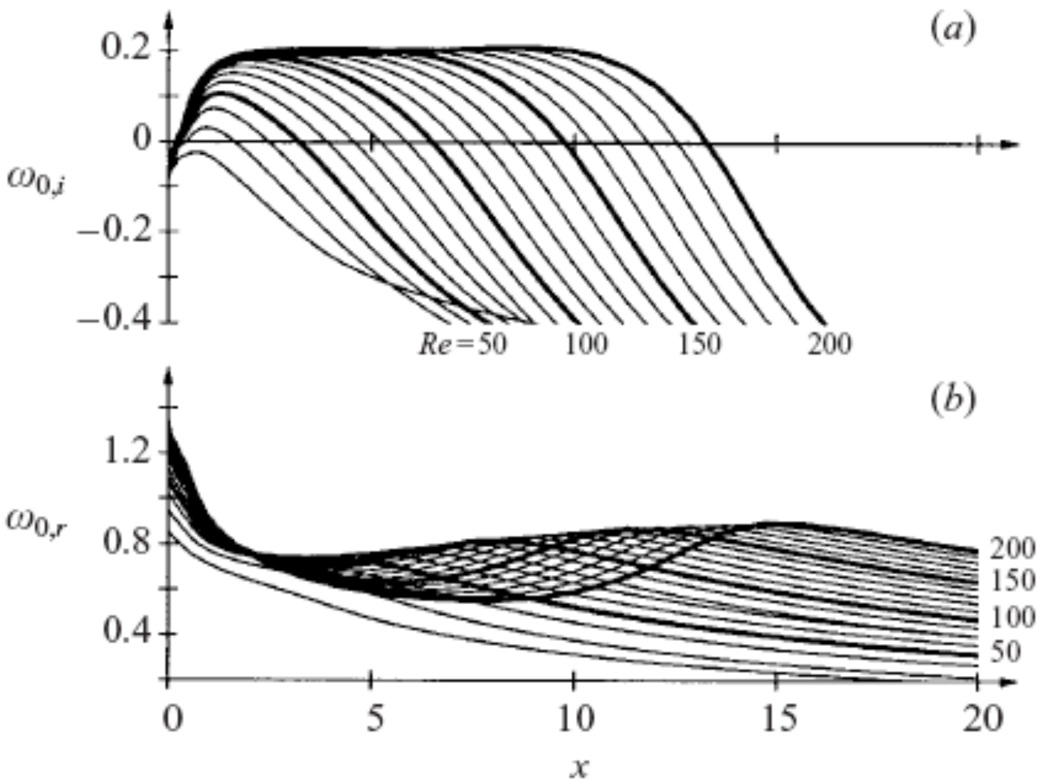

Predictions of growth rate as a function of Reynolds number for the steady cylinder wake.

Predicted wake frequency

Frequency Predictions based on Near-Parallel, Inviscid Assumption

- *Nonlinear theory* **indicates that the saturated wake frequency corresponds to the frequency predicted from the Initial Resonance Criterion (IRC) of Monkewitz and Nguyen (1987) based on** *linear analysis*.

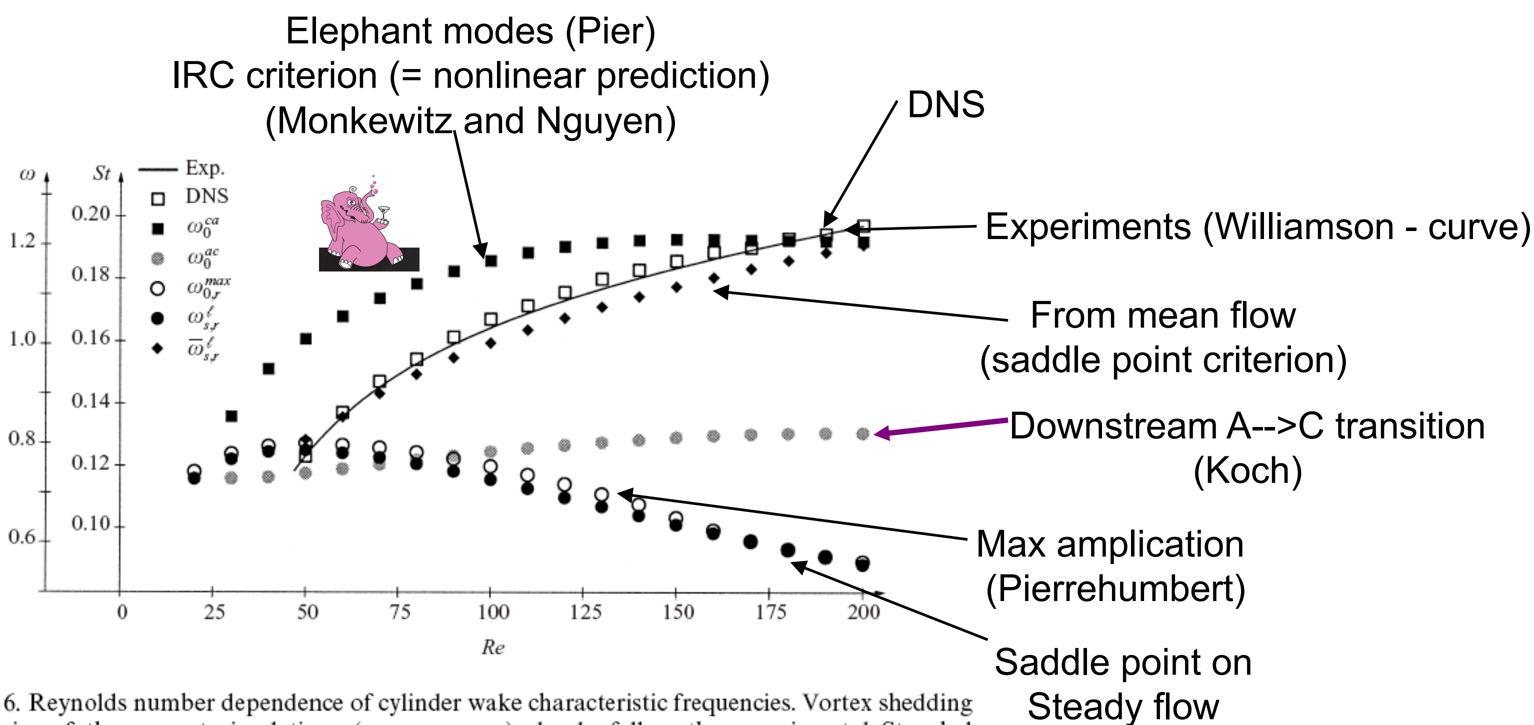

FIGURE 6. Reynolds number dependence of cylinder wake characteristic frequencies. Vortex shedding frequencies of the present simulations (open squares) closely follow the experimental Strouhal number curve from Williamson (1988) (solid line). Theoretical elephant frequencies ω_0^{ca} (filled squares) approximately predict the actual vortex shedding frequencies for $Re > 100$. The other characteristic frequencies ω_0^{ac} (grey circles), $\omega_{0,r}^{max}$ (open circles) and $\omega_{s,r}^{\ell}$ (filled circles) are unable to account for the fully developed vortex street beyond onset at $Re \simeq 49$. Note the good performance of $\bar{\omega}_{s,r}^{\ell}$ based on the mean flow (diamonds).

Global Stability Analysis

- **Prediction based on *Global* instability analysis of time-mean wake. (Barkley 2006).**

Match with experiments & DNS
for wake frequency

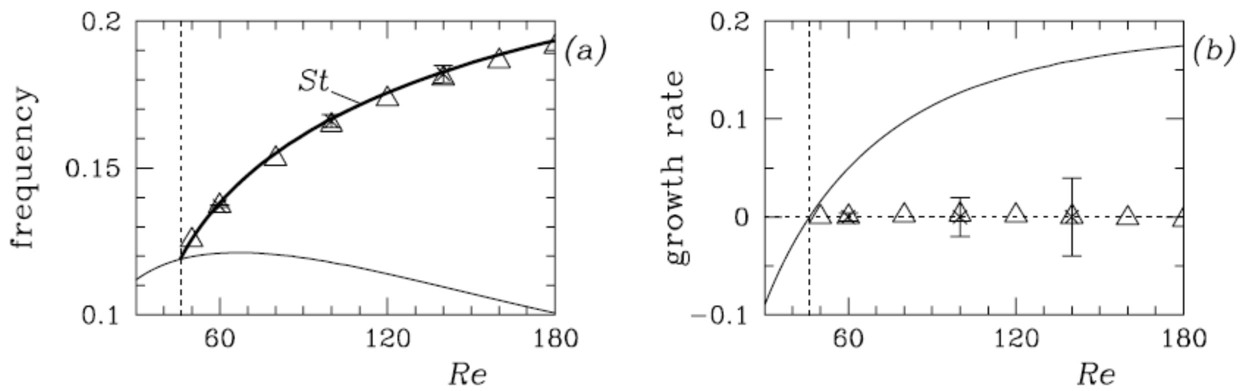

Predicted mode is neutrally stable…

Saddle Point Criterion applied to Higher Re Time-Mean Observations

Low turbulence wind tunnel

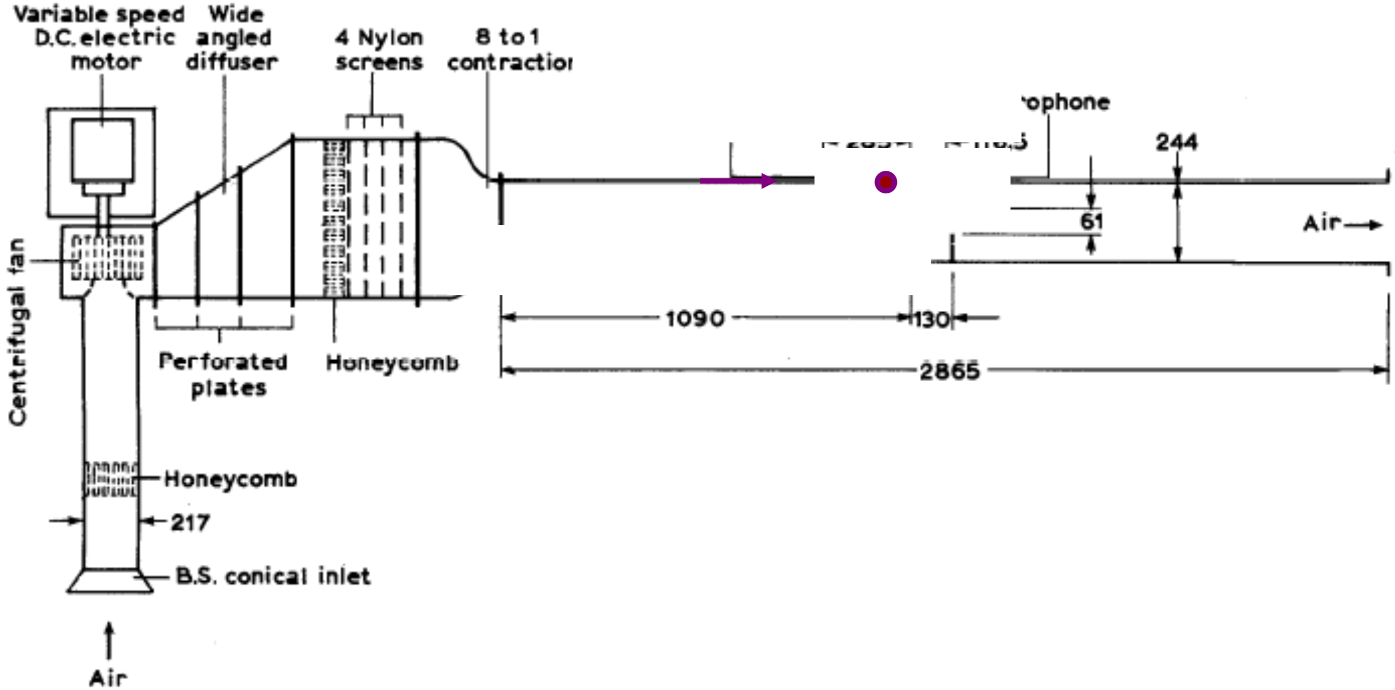

Khor, Sheridan, Thompson & Hourigan, JFM, 2008.

Time-Mean Velocity Profiles & Monkewitz & Nguyen

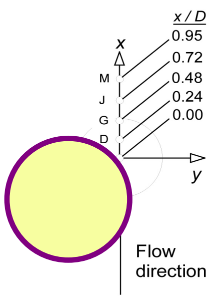

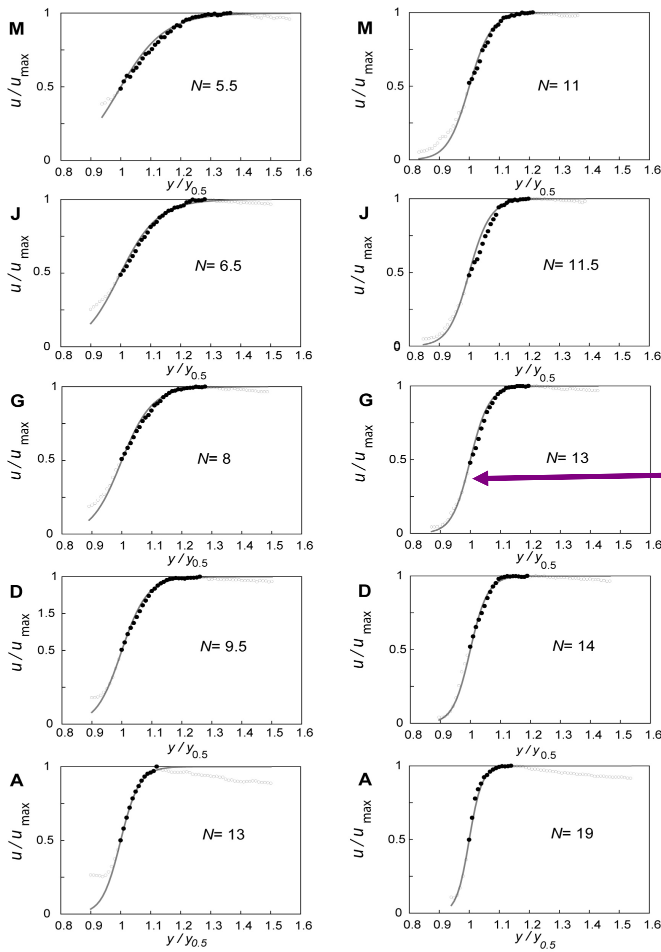

Re = 600

Re = 1700

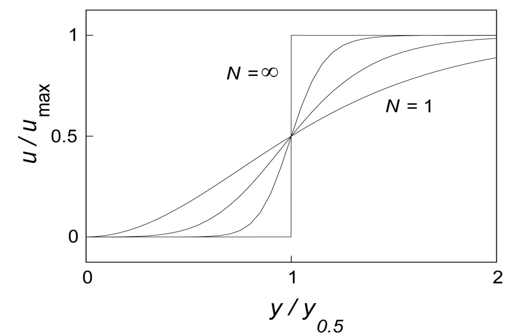

Fit Monkewitz & Nguyen *N* profiles to cylinder wake

$$u(y)/u_{max} = 1 - R + \frac{2R}{1 + \sinh^{2N}\left((y/y_{0.5})\sinh^{-1} 1\right)}$$

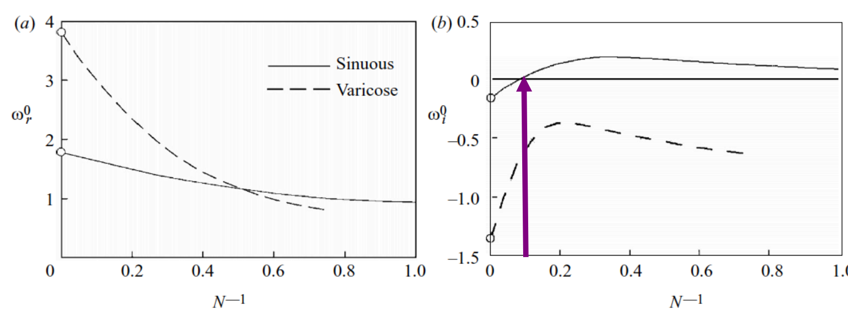

FIGURE 2. The (*a*) real and (*b*) imaginary parts of the branch point frequency of the dispersion relation for the velocity profile (2.1) with $R = -1$, as a function of N^{-1}. After MN.

Positive absolute growth rate $\omega_i^0 > 0$, which indicates absolute instability, for 1/N > 0.08. The corresponding real component of the absolute instability frequency is $\omega_r^0 = 1.68$.

Global Frequency Selection based on Time-Mean Experimental Wake

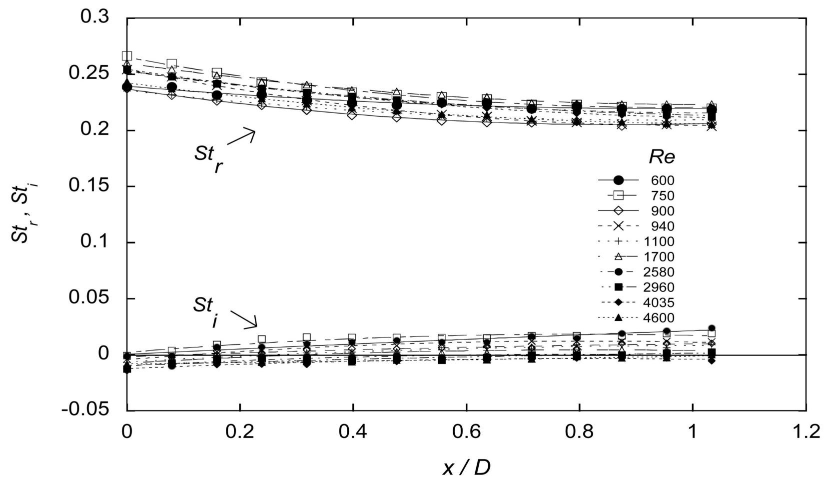

Determine real and imaginary frequencies from stability of each 1/N curve as a function of wake position

Calculate Frequency Selection using Saddle Point Criterion

$$\left.\frac{\partial \omega_0}{\partial x}\right|_{x=x_s} = 0.$$

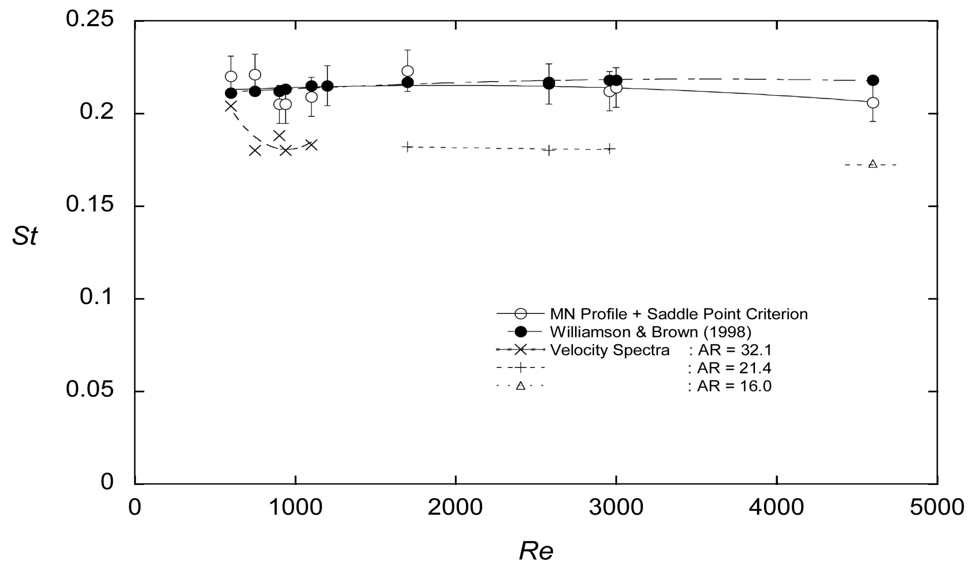

When can the Time-Mean Wake be used for Global Frequency Selection?

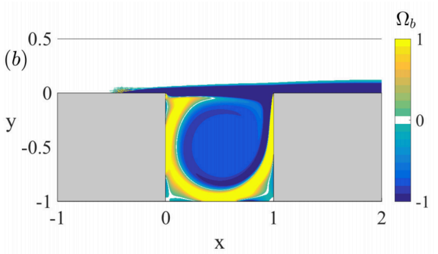

- **Sipp and Lebedev, JFM, 2007.**
  - Two cases: circular cylinder wake and flow over a cavity
  - Two conditions, involving parameters related to the nonlinear interactions in the wake, need to be satisfied:
    - > (a) for the time-mean flow to be approximately marginally stable, and
    - > (b) for the stability of the time-mean flow approximately to yield the nonlinear frequency of the limit cycle.
  - The physical meaning of these two conditions is that the saturation process on the limit cycle is linked to the mean flow harmonic.
  - The circular cylinder satisfies these, the cavity flow does not.

Shear layer and large-scale vortices

Kourta et al., JFM, 1987.

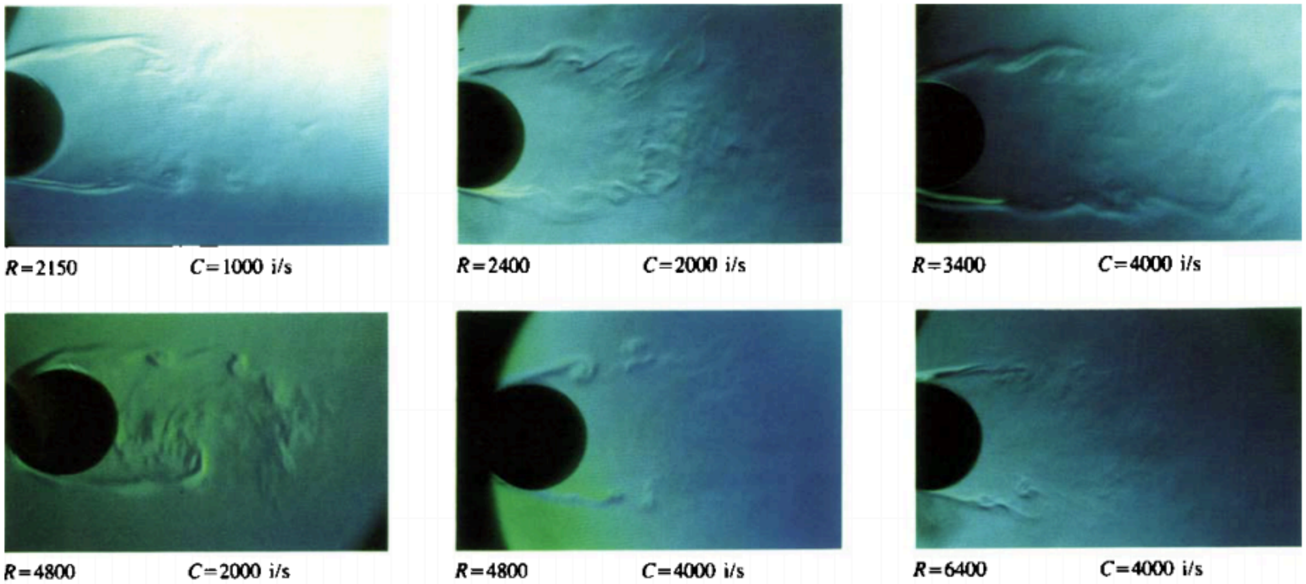

FIGURE 2. Flow visualizations at low Reynolds numbers: $R=U_0D/\nu$; C=camera speed in images per s.

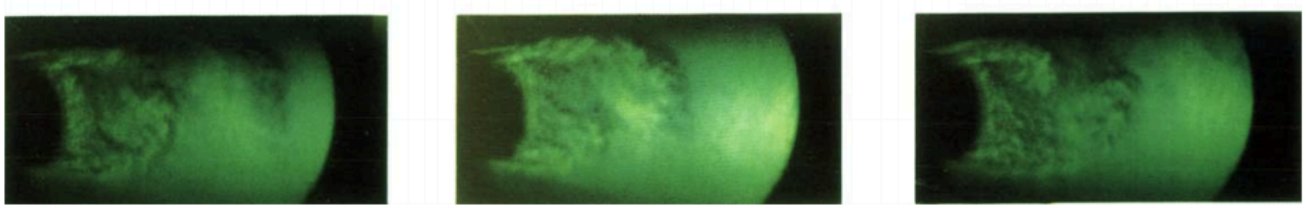

FIGURE 5. Flow visualizations at high Reynolds numbers: R=20 000; C=2000 i/s.

Strong coupling at low Reynolds numbers characterized by phase modulations between the two types of structures; shear layer and large-scale.

2d shear layer instability appears at Re ≈1200

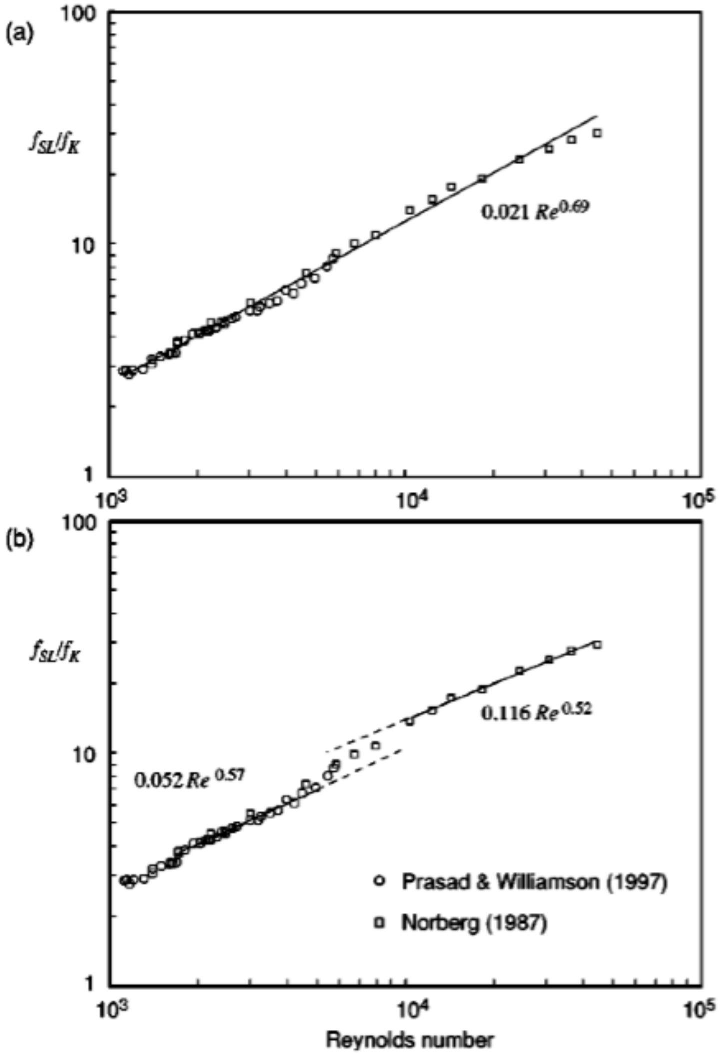

Thompson & Hourigan, PoF, 2005

- Bloor-Gerrard instability persists to high Re
- Global variation of $f_{SL}/f_{BvK} \approx Re^{0.69}$
- Within each step, $f_{SL}/f_{BvK} \approx Re^{0.5}$, as predicted by Bloor (1964) based on separating BL

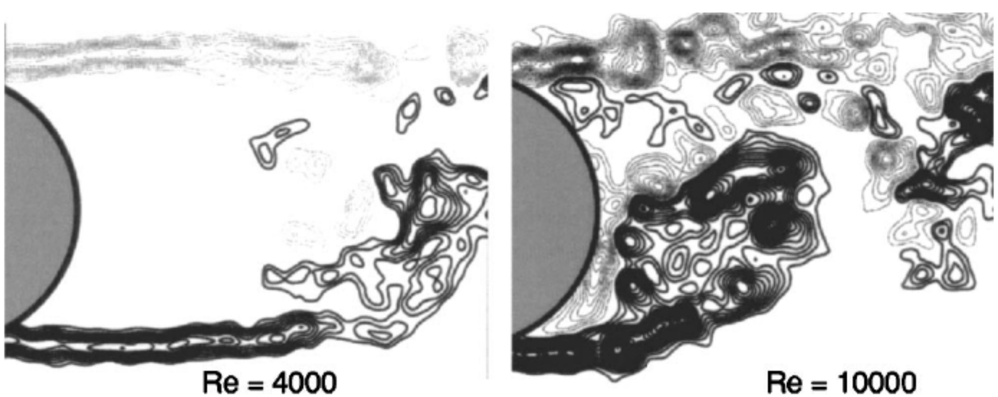

N. Saelim and D. Rockwell, private comm. (2004)

Instabilities form in the far wake

Taneda (1959)
Cimbala, Nagib and Roshko (1988)
Williamson and Prasad (1993)

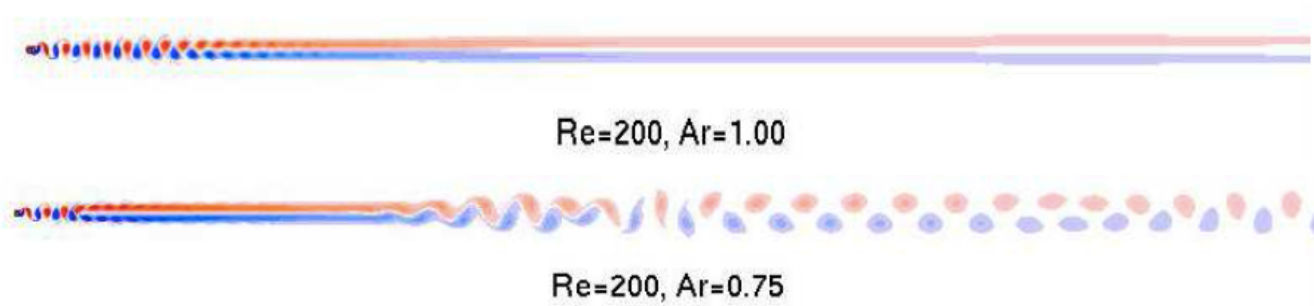

Johnson et al. (2004)
Radi et al. (2013)
Thompson et al. (2014)

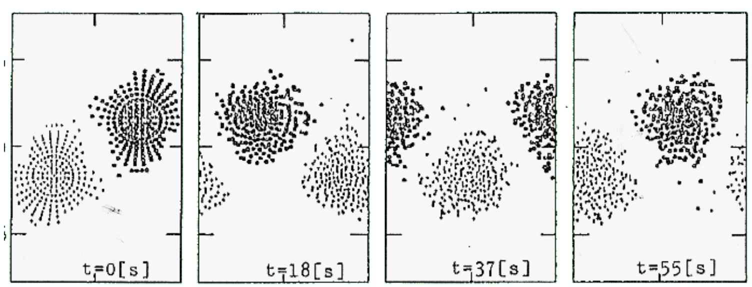

h / a = 0.31

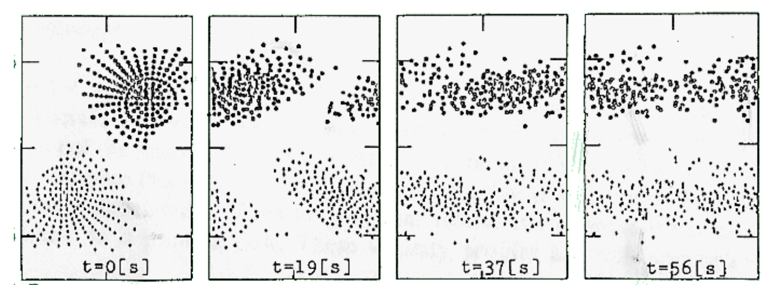

h / a = 0.41

Evolution of vortex street composed of point vortices

Karasudani and Funakoshi (1994)

Linear Stability Analysis: Floquet

Floquet analysis is a linear stability analysis that considers the growth rate of perturbations on the 2D base flow.

Let $U(x, y, t)$ be the 2D wake (base flow) of period T, and $\boldsymbol{u'}(x, y, t)$ be an infinitesimal 3D perturbation to this base flow that evolves according to the linearised Navier-Stokes equations in the computational domain Ω:

$$\frac{\partial \boldsymbol{u'}}{\partial t} = \text{-}\mathbf{DN}\boldsymbol{u'} \text{ - } \frac{1}{\rho}\nabla p' \; + \; \frac{1}{Re}\nabla^2 \boldsymbol{u'} = \mathbf{L}\ (\boldsymbol{u'}) \text{ in } \Omega,$$

$$\nabla \cdot \boldsymbol{u'} = 0 \text{ in } \Omega,$$

where p' is the perturbation to pressure and $\mathbf{DN}\boldsymbol{u'}$ is the linearised advection term:

$$\mathbf{DN}\boldsymbol{u'} \equiv (\boldsymbol{u'} \cdot \nabla)\, \boldsymbol{U} + (\boldsymbol{U} \cdot \nabla)\, \boldsymbol{u'}.$$

The perturbed flow $\boldsymbol{U} + \boldsymbol{u'}$ satisfies the same boundary conditions as the base flow. The operator $\mathbf{L}\ (\boldsymbol{u'})$ in the equation $\dfrac{\partial \boldsymbol{u'}}{\partial t} = \mathbf{L}\ (\boldsymbol{u'})$ is T-periodic and is of the Floquet type.

Solutions of this equation can be decomposed in to a sum of solutions of the form: $\tilde{\boldsymbol{u}}(x, y, t)exp(\sigma t)$. The complex numbers σ are the Floquet exponents, but often the Floquet multipliers $\mu \equiv exp(\sigma T)$ are used. Multipliers outside the unit circle $(|\mu|) > 1)$ correspond to exponentially growing solutions $(\text{Re } \sigma > 0)$.

Floquet Analysis of wake of circular cylinder

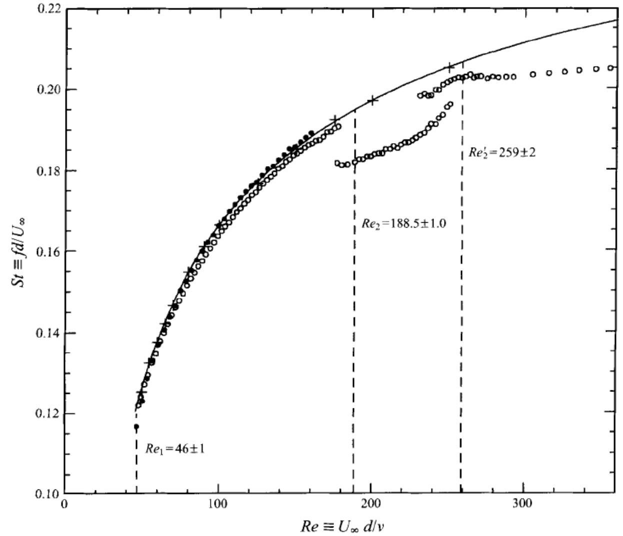

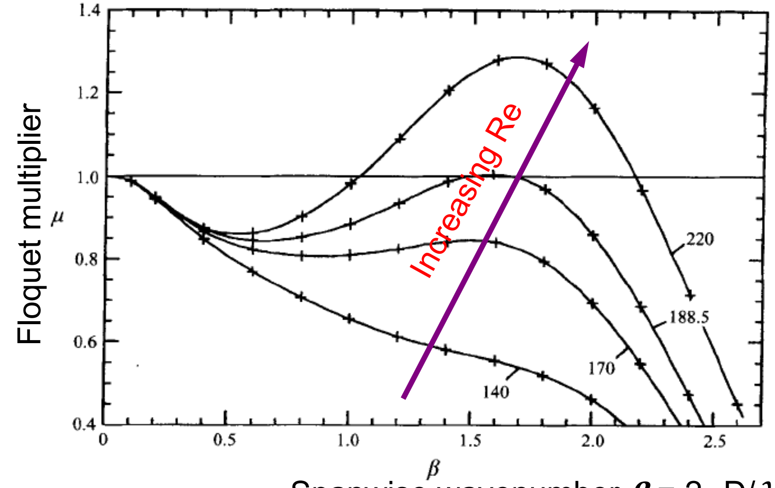

Spanwise wavenumber $\boldsymbol{\beta} = 2\boldsymbol{\pi}D/\boldsymbol{\lambda}$

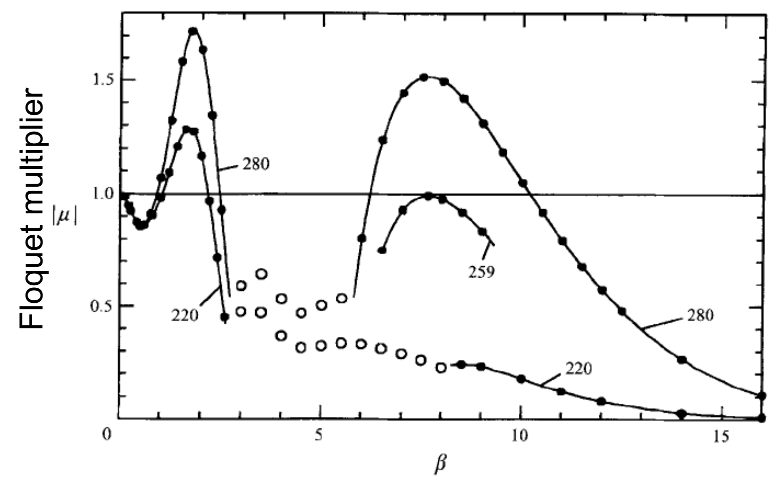

Spanwise wavenumber $\boldsymbol{\beta} = 2\boldsymbol{\pi}D/\boldsymbol{\lambda}$

Barkley & Henderson, JFM (322), 1996.

Conclusions

- There can be a number of transitions in the wakes of bluff bodies, including:
  Flow separation
  Separating shear layer instability
  Large-scale vortex shedding
  Three-dimensional vortex formation
  Wake relaminarization and secondary wake

- Various techniques for investigating wake instabilities:
    - Linear:
        - Rayleigh/Orr Sommerfeld
        - Saddle point
        - Floquet
    - Nonlinear

- All involve assumptions – need to be careful in interpretation